UC Santa Barbara
UC Santa Barbara Previously Published Works

Title

Correlation between stoichiometry, strain, and metal-insulator transitions of NdNiO$_3$ films

Authors

Hauser, Adam J
Mikheev, Evgeny
Moreno, Nelson E
et al.

Peer reviewed

Correlation between stoichiometry, strain, and metal-insulator transitions of NdNiO3 films

Adam J. Hauser, Evgeny Mikheev, Nelson E. Moreno, Jinwoo Hwang, Jack Y. Zhang, and Susanne Stemmer

---

Articles you may be interested in

Anisotropic-strain-controlled metal-insulator transition in epitaxial NdNiO3 films grown on orthorhombic NdGaO3 substrates
Appl. Phys. Lett. **103**, 172110 (2013); 10.1063/1.4826678

Strain controlled systematic variation of metal-insulator transition in epitaxial NdNiO3 thin films
J. Appl. Phys. **112**, 073718 (2012); 10.1063/1.4758306

Probing the metal-insulator transition of NdNiO3 by electrostatic doping
Appl. Phys. Lett. **99**, 192107 (2011); 10.1063/1.3659310

Nd 0.8 Y 0.2 NiO 3 thin films with room-temperature metal–insulator transition deposited by pulsed laser ablation
J. Appl. Phys. **93**, 5136 (2003); 10.1063/1.1563815

Strain-induced tuning of metal–insulator transition in NdNiO 3
Appl. Phys. Lett. **80**, 4039 (2002); 10.1063/1.1480475

CrossMark
click for updates

Correlation between stoichiometry, strain, and metal-insulator transitions of NdNiO$_3$ films

Adam J. Hauser, Evgeny Mikheev, Nelson E. Moreno, Jinwoo Hwang, Jack Y. Zhang, and Susanne Stemmer

Materials Department, University of California, Santa Barbara, California 93106-5050, USA

The interplay of film stoichiometry and strain on the metal-insulator transition (MIT) and Hall coefficient of NdNiO$_3$ films grown under different conditions is investigated. Unstrained lattice parameters and lattice mismatch strains are evaluated for films grown under a range of growth pressures and on different substrates. It is shown that both the temperature of the MIT and the Hall coefficient in the metallic phase are highly sensitive to film strain. In films grown with lower oxygen/total growth pressures, very large compressive in-plane strains can be obtained, which can act to suppress the MIT. Both the Hall coefficient and the temperature of the MIT are relatively insensitive to growth pressure, provided that films under the same strain are compared. The results support an itinerant picture of the transition that is controlled by the Ni e$_g$ bands, and that is relatively insensitive to changes in film stoichiometry. © 2015 AIP Publishing LLC.
[http://dx.doi.org/10.1063/1.4914002]

The rare earth nickelates (RNiO$_3$, where R is a trivalent rare earth ion but not La) exhibit a prototype, bandwidth-controlled Mott metal-insulator transition (MIT).[1–3] Predictions of emergent states in quantum confined RNiO$_3$ heterostructures[4] and interest in controlling the MIT with applied electric fields[5–8] have resulted in renewed efforts to achieve a more complete understanding of the MIT.[9–12] One important question concerns the importance of charge transfer from the oxygens to the Ni, i.e., from the formal d^7 electron configuration on the Ni sites to one that is closer to d^8 with holes on the oxygens.[12] In this picture, one proposal for the nature of the transition is that of a site-selective, strongly correlated Mott insulator.[13] A different understanding of the MIT is one that starts with an itinerant electron system in which the transition is controlled by the Fermiology of the Ni d-bands, with little direct influence from the oxygen p-orbitals (although hybridization does, of course, exist).[9,10] Recent x-ray resonant scattering that show spin density waves[14] and tunneling experiments that detect a pseudogap[15] suggest that an itinerant picture applies well into the insulating phase.

RNiO$_3$ heterostructures offer unique probes of the MIT. For example, it is well established that coherency strains shift the MIT transition temperature (T_{MIT}) and can even completely suppress it.[16–20] T_{MIT} is sensitive to Ni-O bond lengths and changes in the Ni-O-Ni bond angles,[3] which are modified by the lattice mismatch strain. A quantitative understanding exists in the literature of the specific modification of bond angles and lengths under biaxial stress.[21–24] Changes in T_{MIT} due to bond angles and lengths are consistent with the general understanding of a bandwidth-controlled MIT. Results in the literature are, however, often somewhat inconsistent. For example, for NdNiO$_3$ films on LaAlO$_3$ substrates, some studies observe a complete suppression of the MIT,[17,18] while others do not.[19,20,25] Synthesis of oxygen stoichiometric, single-phase RNiO$_3$ requires high oxygen pressures.[26] Disorder can cause MITs in ultrathin films whose resistance exceeds the

Mott-Ioffe-Regel limit.[27] Here, we systematically study the relative roles of deposition conditions and film strain on the MIT in NdNiO$_3$ films. We show that film strain is the key factor in controlling the MIT, whereas even significant amounts of non-stoichiometry do not appear to influence T_{MIT} or the Hall coefficient in the metallic phase.

Epitaxial NdNiO$_3$ films were grown on different substrates that impart a range of epitaxial lattice mismatches: (110)$_o$YAlO$_3$, (001)$_{pc}$LaAlO$_3$, (110)$_o$NdGaO$_3$, (001)$_c$LSAT, (001)$_c$SrTiO$_3$, and (110)$_o$DyScO$_3$. The subscripts indicate the orthorhombic (o), pseudocubic (pc), and cubic (c) unit cells, respectively. In the following, we use pseudo-cubic unit cells for all films and substrates. Films were grown by RF magnetron sputtering in an Ar/O$_2$ sputter gas mixture.[28] The total growth pressure was varied between 9 and 300 mTorr, and the other growth parameters (sputter gas and RF power) were optimized for each growth pressure, using the structural and electrical properties of the films. Film stoichiometries were determined using Rutherford backscattering (RBS) at the Laboratory for Surface Modification at Rutgers University and analyzed using the SIMNRA program.[29] High-resolution x-ray diffraction (XRD) measurements, atomic-force microscopy, and high-angle annular dark-field (HAADF) scanning transmission electron microscopy (STEM) were performed to determine film and surface structure and lattice parameters. Off-axis XRD ($\Psi = 45°$ with respect to the surface normal) around the 011 reflections was used to extract d_{011} and calculate the in-plane lattice parameter $a_{||} = a_\perp \tan[\sin^{-1}(d_{011}/c)]$. Films were patterned into van der Pauw and Hall bar structures (300 μm channel width) via contact lithography. Ohmic contacts of Ni(20 nm)/Au(300 nm) were deposited by electron beam evaporation, and device isolation was achieved with a wet etch of 25% HCl in water. Measurements of the in-plane longitudinal (R_{xx}) and Hall (R_{xy}) resistances as a function of temperature were performed using a Quantum Design Physical Properties Measurement System (PPMS). R_{xx} was measured between

300 K and 2 K upon cooling and heating. R_{xy} and R_{xx} were measured simultaneously from 200 K to 20 K, using a magnetic field (B) sweeps between ± 9 T. Below T_{MIT}, the Hall coefficient, R_H, must be corrected for the time-dependence of R_{xx}, as discussed previously.[25] Hall measurements are reported for each sample at temperatures in which we can reasonably perform drift-correction, i.e., temperatures in which the parasitic magnetoresistance is not significantly larger than the Hall signal.

A representative example of the effect of growth pressure and mismatch strain on the films' lattice parameters is shown in Fig. 1 for the films grown on LaAlO$_3$. The
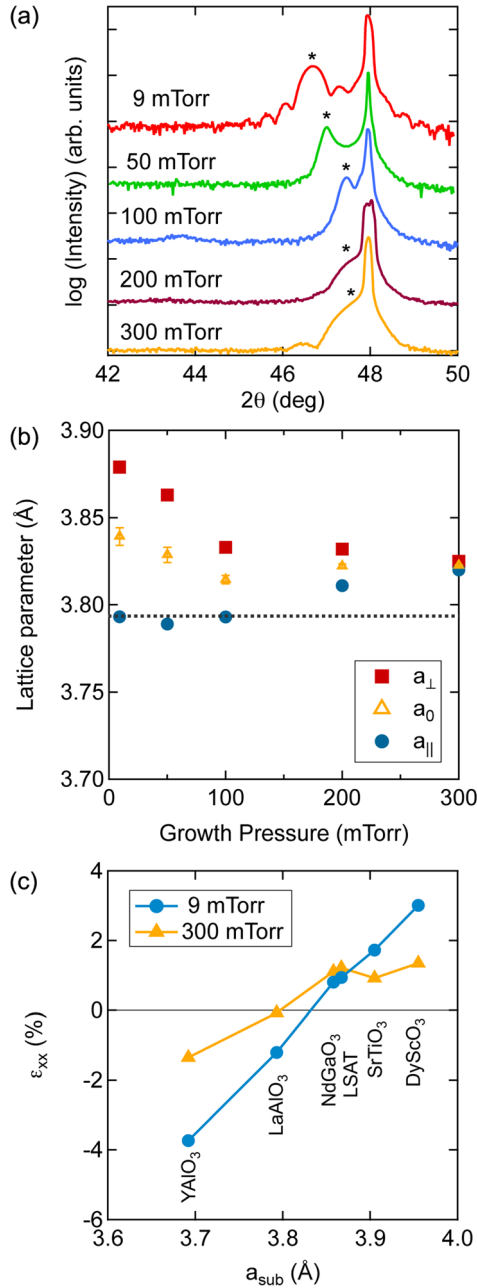

FIG. 1. (a) On-axis XRD of NdNiO$_3$ on LaAlO$_3$ for different total growth pressures. The asterisks indicate the film peaks. (b) Measured $a_\perp$ (solid red squares) and $a_\parallel$ (solid green circles), and calculated a_0 (open orange triangles) as a function of growth pressure. The grey line indicates the lattice parameter of LaAlO$_3$ (3.79 Å). (c) In-plane film strain as a function of substrate lattice parameter for two different growth pressures, calculated as $\varepsilon_{xx} = (a_\parallel - a_0)/a_0$.

out-of-plane NdNiO$_3$ lattice spacing ($a_\perp$) decreases with increasing growth pressure [Fig. 1(a)]. Figure 1(b) shows that the films are coherently strained to the substrate at lower growth pressures ($a_\parallel = a_{LaAlO_3}$) and (partially) relaxed at higher pressures ($a_\parallel \neq a_{LaAlO_3}$). It is important to note that values for $a_\parallel$ and $a_\perp$ do not change appreciably between 6 and 17 nm for a particular substrate choice or growth conditions. Furthermore, the unstrained film lattice parameter (a_0) was determined as function of growth pressure and substrate, as given by

$$a_0 = \frac{2va_\parallel + (1 - v)a_\perp}{1 + v}, \qquad (1)$$

where v is the Poisson's ratio, which was set to 0.3 here in the absence of any information about the elastic constants of NdNiO$_3$. Films grown at high pressures were not phase-pure, and a_0 is the lattice parameter of the (non)stoichiometric perovskite phase, with effects on the lattice parameter from coherency strains removed. At lower total growth pressures, a_0 is increased relative to the bulk pseudocubic value of 3.81 Å[30] and also larger than that of high pressure films. It is well known that in the nickelates oxygen deficiency results in an expanded lattice parameter.[31,32] It is also possible that the lower growth pressures resulted in the cation nonstoichiometry without giving rise to secondary phases (as are observed in Ni-rich films), and this also may affect a_0.

Figure 1(c) shows the film strain for all substrates for the films grown at 9 and 300 mTorr total pressures, as a function of substrate lattice parameter. The in-plane film strain, ε_{xx}, was calculated as $\varepsilon_{xx} = (a_\parallel - a_0)/a_0$, using the unstrained film lattice parameter determined as described above. As a result of the different intrinsic lattice parameters, ε_{xx} is different for films grown under low and high pressures, respectively, on the same substrate. Furthermore, high-pressure films are (partially) relaxed for substrates that have a large lattice mismatch, resulting in smaller ε_{xx} values. The absolute ε_{xx} values that can be achieved are much larger for the low-pressure films. For example, on LaAlO$_3$, the high-pressure films are almost fully relaxed ($\varepsilon_{xx} \sim -0.07\%$), while the low-pressure films are under an extremely large strain (-1.2%). Films grown at higher pressure are Ni-rich [see RBS data shown in Fig. 2(a)]. The excess Ni is accommodated in form of NiO precipitates [Fig. 2(b)], which occur mostly at the surface for the 300 mTorr films. As shown below, the NiO particles do not measurably influence T_{MIT}. We note that in Figure 1(b), the broad peak at $2\theta = 43°-44°$ in the 100 mTorr film corresponds to a NiO phase. At 100 mTorr, films have similar Ni/Nd ratios but do phase separate in the form of round NiO particles, forming a stripe pattern instead (Figure S2 in the supplementary material). No precipitates or striping were found in the 9 mTorr films, consistent with a Ni/Nd ratio near 1.

Figure 3(a) shows the film resistivities as a function of temperature for the films on NdGaO$_3$ ($a_{pc} = 3.86$ Å) and LaAlO$_3$ ($a = 3.79$ Å), respectively, for the low and high pressure films. Note that NdGaO$_3$ has the smallest mismatch (tensile), while LaAlO$_3$ puts the films under compressive strain [see Fig. 1(c)]. The resistivities at 300 K are almost
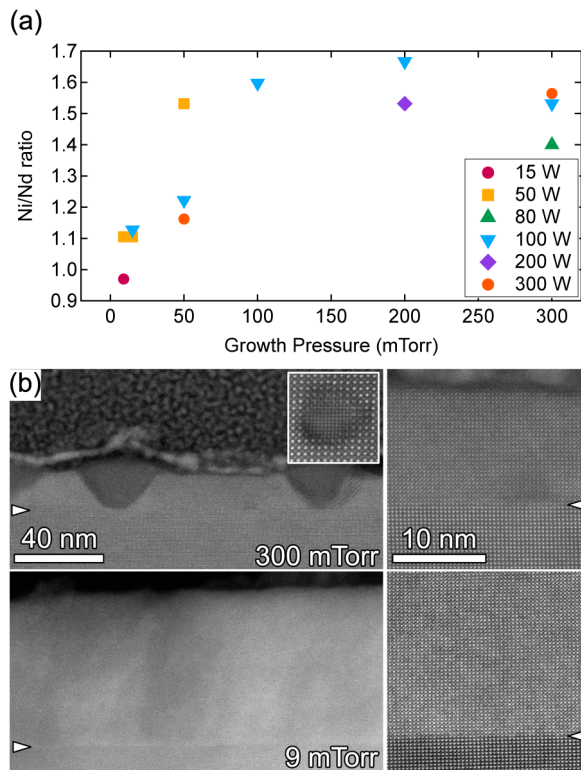
FIG. 2. (a) Ni/Nd ratios as a function of total growth pressure measured by RBS for different RF sputter powers. (b) STEM cross-section images of NdNiO$_3$ films on LaAlO$_3$ grown at total growth pressures of 300 mTorr (top) and 9 mTorr (bottom). The inset shows a plan view image of a NiO inclusion. Arrows indicate the NdNiO$_3$/LaAlO$_3$ interface.
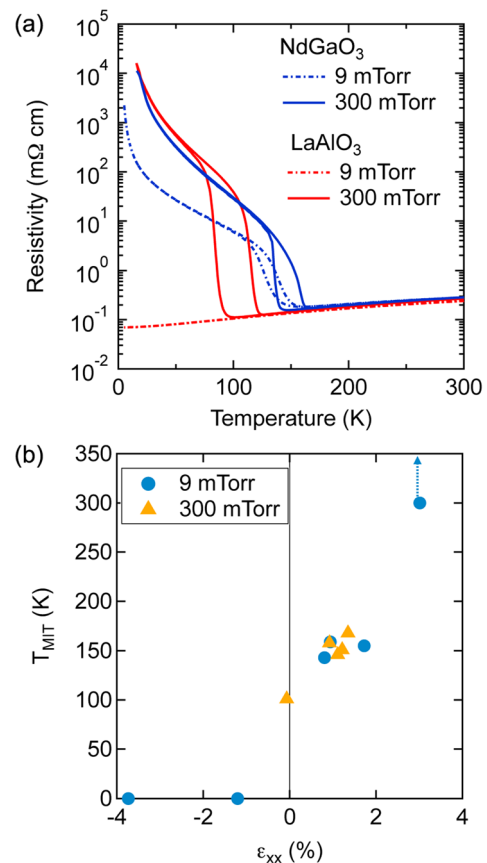

FIG. 3. (a) Film resistivities as a function of temperature for NdNiO$_3$ thin films on two different substrates and grown at different pressures. (b) T_{MIT} as a function of ε_{xx} for film grown at total growth pressures of 300 mTorr and 9 mTorr. The arrow (on the data point for the film on the DyScO$_3$ substrate) indicates that this film is insulating at all temperatures below 300 K.

independent of mismatch strain and are around 2×10^{-4} Ω cm, which is similar to the best bulk materials.[33] In contrast, T_{MIT} is strongly affected. In particular, for films grown at low pressure, no MIT is observed for the films on LaAlO$_3$ and YAlO$_3$, which are under a large compressive strain. In contrast, films grown at high pressure still show a MIT on both substrates. The relationship between film strain and T_{MIT} can be seen more clearly from Fig. 3(b), which shows T_{MIT} (taken here as the minimum temperature in the $R_{xx}(T)$ curves) as a function of ε_{xx}. T_{MIT} of all films, *irrespective of their stoichiometry*, is essentially determined by the film strain.

Figure 4 shows the results of the time-corrected Hall measurements for NdGaO$_3$ and LaAlO$_3$ substrates. In general (not shown), the high pressure films showed a more time dependent behavior and also a sharper transition [as defined, for example, by $R_{xx}(50\,\text{K})/R_{xx}(200\,\text{K})$] than the low pressure films and both were dependent on strain. Both phenomena are associated with the kinetics of metallic and insulating domains. As has been observed previously, the MIT is associated with a crossover from positive R_H at high temperatures to a negative R_H at low temperatures. Since T_{MIT} depends on the different film strains, we show the temperature relative to that of the crossover temperature. Well above T_{MIT}, nearly identical R_H values are obtained for films grown on NdGaO$_3$, regardless of growth pressure, and R_H is nearly independent of temperature. The relaxed, high-pressure film on LaAlO$_3$ yields an R_H in the metallic phase that is 20 times lower than films grown on NdGaO$_3$.

The results shown here allow for insights into the MIT of NdNiO$_3$. First, NdNiO$_3$ films with significant differences in the film stoichiometry show robust MITs that appear to be relatively insensitive to cation stoichiometry or the oxygen partial pressure during growth. T_{MIT} is similar for films grown at high and low pressures, provided that they are under similar mismatch strain [Figs. 3(b) and 4]. The main
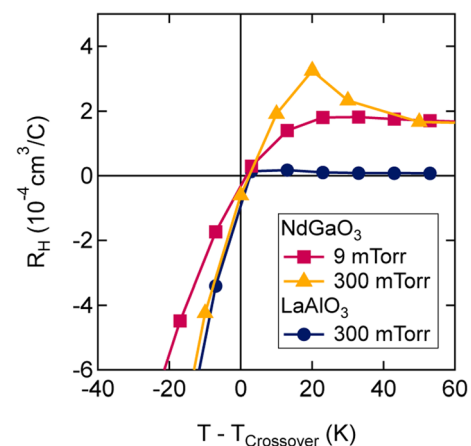

FIG. 4. R_H as a function of temperature relative to the temperature at which R_H changes sign.

parameter that influences the T_{MIT} and R_H is film strain. Differences appear mainly because the low-pressure films can be coherently strained to larger strains than the high-pressure films, which are (partially) relaxed on the substrates that have the largest mismatch. At present, we do not have an understanding why films grown at low pressure can be strained to larger strains without relaxing. A complete suppression of the MIT can be achieved in low-pressure films that are under a very large compressive strain. The results explain the different results for T_{MIT} obtained in the literature on the same substrates with differences in film strain caused by differences in the intrinsic film lattice parameter.

It is important to revisit the fact that T_{MIT} of $NdNiO_3$ appears to be relatively insensitive to changes the oxygen partial pressure in the growth environment. The oxygen partial pressure also does not appear to have a noticeable influence on R_H in the metallic phase. Thus, any possible increase in oxygen vacancies, which we may consider as equivalent to electron doping the Ni e_g states, does not seem to have a large effect on the mobile carriers or Fermi surfaces. This is different from results of studies in which Nd is replaced with a divalent cation, which causes a suppression of T_{MIT}.[34,35] While the sign of R_H in the insulating phase can be ambiguous,[36] the positive R_H of the metallic nickelates is understood as being dominated by the large hole surface that overwhelms the contribution of the smaller electron pocket; both are derived from the Ni e_g states.[25,37–40] The results indicate that changes in stoichiometry do not influence the electronic states that are relevant for the MIT nor do they appear to significantly change the relative e_g Fermi surface areas, consistent with the findings on $LaNiO_3$ superlattices.[41] This supports an itinerant picture of the MIT in $NdNiO_3$[9,10] that is dominated by Ni e_g bands, with little direct influence from the oxygen $2p$ states. In contrast, strain has a large influence on the electronic structure, as reflected in R_H above the MIT. Specifically, in the (almost) unstrained case of the high-pressure film on $LaAlO_3$, R_H is nearly compensated, indicating that the electron pocket and hole surfaces make comparable contributions to R_H. The increase in hole surface under in-plane tensile strain, as reflected in the large positive R_H, is consistent with the recent photoemission results from tensile-strained $LaNiO_3$ films, which show a large flat hole surface,[42] similar changes in R_H for $LaNiO_3$ films,[43] and x-ray absorption studies that show a large change in orbital polarization under strain.[41] The results show that a large hole Fermi surface stabilizes the insulating state in $NdNiO_3$ (shifting T_{MIT} to higher temperatures), possibly by promoting Fermi surface nesting and a spin density wave.[9,10]

[1] J. B. Torrance, P. Lacorre, A. I. Nazzal, E. J. Ansaldo, and C. Niedermayer, Phys. Rev. B **45**, 8209 (1992).
[2] P. C. Canfield, J. D. Thompson, S. W. Cheong, and L. W. Rupp, Phys. Rev. B **47**, 12357 (1993).
[3] J. S. Zhou and J. B. Goodenough, Phys. Rev. B **69**, 153105 (2004).
[4] J. Chaloupka and G. Khaliullin, Phys. Rev. Lett. **100**, 016404 (2008).
[5] R. Scherwitzl, P. Zubko, I. G. Lezama, S. Ono, A. F. Morpurgo, G. Catalan, and J.-M. Triscone, Adv. Mater. **22**, 5517 (2010).
[6] S. Asanuma, P.-H. Xiang, H. Yamada, H. Sato, I. H. Inoue, A. Sawa, K. Ueno, H. Shimotani, H. Yuan *et al.*, Appl. Phys. Lett. **97**, 142110 (2010).
[7] J. Son, B. Jalan, A. P. Kajdos, L. Balents, S. J. Allen, and S. Stemmer, Appl. Phys. Lett. **99**, 192107 (2011).
[8] J. Son, S. Rajan, S. Stemmer, and S. J. Allen, J. Appl. Phys. **110**, 084503 (2011).
[9] S. Lee, R. Chen, and L. Balents, Phys. Rev. Lett. **106**, 016405 (2011).
[10] S. B. Lee, R. Chen, and L. Balents, Phys. Rev. B **84**, 165119 (2011).
[11] B. Lau and A. J. Millis, Phys. Rev. Lett. **110**, 126404 (2013).
[12] T. Mizokawa, D. I. Khomskii, and G. A. Sawatzky, Phys. Rev. B **61**, 11263 (2000).
[13] H. Park, A. J. Millis, and C. A. Marianetti, Phys. Rev. Lett. **109**, 156402 (2012).
[14] A. Frano, E. Schierle, M. W. Haverkort, Y. Lu, M. Wu, S. Blanco-Canosa, U. Nwankwo, A. V. Boris, P. Wochner, G. Cristiani *et al.*, Phys. Rev. Lett. **111**, 106804 (2013).
[15] S. J. Allen, A. J. Hauser, E. Mikheev, J. Y. Zhang, N. E. Moreno, J. Son, D. G. Ouellette, J. Kally, A. Kozhanov, L. Balents *et al.*, e-print arXiv:1404.2544 [cond-mat.str-el].
[16] G. Catalan, R. M. Bowman, and J. M. Gregg, Phys. Rev. B **62**, 7892 (2000).
[17] J. A. Liu, M. Kareev, B. Gray, J. W. Kim, P. Ryan, B. Dabrowski, J. W. Freeland, and J. Chakhalian, Appl. Phys. Lett. **96**, 233110 (2010).
[18] A. S. Disa, D. P. Kumah, J. H. Ngai, E. D. Specht, D. A. Arena, F. J. Walker, and C. H. Ahn, APL Mater. **1**, 032110 (2013).
[19] M. A. Novojilov, O. Y. Gorbenko, I. E. Graboy, A. R. Kaul, H. W. Zandbergen, N. A. Babushkina, and L. M. Belova, Appl. Phys. Lett. **76**, 2041 (2000).
[20] P. H. Xiang, N. Zhong, C. G. Duan, X. D. Tang, Z. G. Hu, P. X. Yang, Z. Q. Zhu, and J. H. Chu, J. Appl. Phys. **114**, 243713 (2013).
[21] S. J. May, J. W. Kim, J. M. Rondinelli, E. Karapetrova, N. A. Spaldin, A. Bhattacharya, and P. J. Ryan, Phys. Rev. B **82**, 014110 (2010).
[22] J. Hwang, J. Y. Zhang, J. Son, and S. Stemmer, Appl. Phys. Lett. **100**, 191909 (2012).
[23] I. C. Tung, P. V. Balachandran, J. Liu, B. A. Gray, E. A. Karapetrova, J. H. Lee, J. Chakhalian, M. J. Bedzyk, J. M. Rondinelli, and J. W. Freeland, Phys. Rev. B **88**, 205112 (2013).
[24] A. Vailionis, H. Boschker, W. Siemons, E. P. Houwman, D. H. A. Blank, G. Rijnders, and G. Koster, Phys. Rev. B **83**, 064101 (2011).
[25] A. J. Hauser, E. Mikheev, N. E. Moreno, T. A. Cain, J. Hwang, J. Y. Zhang, and S. Stemmer, Appl. Phys. Lett. **103**, 182105 (2013).
[26] M. Zinkevich and F. Aldinger, J. Alloys Compd. **375**, 147 (2004).
[27] J. Son, P. Moetakef, J. M. LeBeau, D. Ouellette, L. Balents, S. J. Allen, and S. Stemmer, Appl. Phys. Lett. **96**, 062114 (2010).
[28] See supplemental material at http://dx.doi.org/10.1063/1.4914002 for film growth parameters and optimization, additional data for lattice parameters as a function of growth conditions, and additional TEM images.
[29] M. Mayer, "IMNRA User's Guide," Max-Planck-Institut fur Plasmaphysik Report No. Report IPP 9/113, Garching, Germany, 1997.
[30] J. L. García-Muñoz, J. Rodriguez-Carvajal, P. Lacorre, and J. B. Torrance, Phys. Rev. B **46**, 4414 (1992).
[31] S. D. Ha, M. Otaki, R. Jaramillo, A. Podpirka, and S. Ramanathan, J. Solid State Chem. **190**, 233 (2012).
[32] I. V. Nikulin, M. A. Novojilov, A. R. Kaulb, S. N. Mudretsovab, and S. V. Kondrashov, Mater. Res. Bull. **39**, 775 (2004).
[33] J. S. Zhou, J. B. Goodenough, and B. Dabrowski, Phys. Rev. Lett. **94**, 226602 (2005).

[34] J. L. García-Muñoz, M. Suaaidi, M. J. Martínez-Lope, and J. A. Alonso, Phys. Rev. B **52**, 13563 (1995).

[35] S. W. Cheong, H. Y. Hwang, B. Batlogg, A. S. Cooper, and P. C. Canfield, Physica B **194**, 1087 (1994).

[36] T. Holstein, Philos. Mag. **27**, 225 (1973).

[37] R. Eguchi, A. Chainani, M. Taguchi, M. Matsunami, Y. Ishida, K. Horiba, Y. Senba, H. Ohashi, and S. Shin, Phys. Rev. B **79**, 115122 (2009).

[38] N. Hamada, J. Phys. Chem. Solids **54**, 1157 (1993).

[39] S. D. Ha, R. Jaramillo, D. M. Silevitch, F. Schoofs, K. Kerman, J. D. Baniecki, and S. Ramanathan, Phys. Rev. B **87**, 125150 (2013).

[40] P. D. C. King, H. I. Wei, Y. F. Nie, M. Uchida, C. Adamo, S. Zhu, X. He, I. Bozovic, D. G. Schlom, and K. M. Shen, Nat. Nanotechnol. **9**, 443 (2014).

[41] M. Wu, E. Benckiser, M. W. Haverkort, A. Frano, Y. Lu, U. Nwankwo, S. Brück, P. Audehm, E. Goering, S. Macke *et al.*, Phys. Rev. B **88**, 125124 (2013).

[42] H. K. Yoo, S. I. Hyun, L. Moreschini, H.-D. Kim, Y. J. Chang, C. H. Sohn, D. W. Jeong, S. Sinn, Y. S. Kim, A. Bostwick *et al.*, e-print arXiv:1406.2433v1 [cond-mat.str-el].

[43] J. Chakhalian, J. M. Rondinelli, J. Liu, B. A. Gray, M. Kareev, E. J. Moon, N. Prasai, J. L. Cohn, M. Varela, I. C. Tung *et al.*, Phys. Rev. Lett. **107**, 116805 (2011).